Inorg. Chem. **2005**, *44*, 1611–1618

Efficient Electroluminescence from New Lanthanide (Eu^{3+}, Sm^{3+}) Complexes

Jiangbo Yu,[†,‡] Liang Zhou,[†] Hongjie Zhang,*[,†] Youxuan Zheng,[†] Huanrong Li,[†] Ruiping Deng,[†,‡] Zeping Peng,[†,‡] and Zhefeng Li[†,‡]

Key Laboratory of Rare Earth Chemistry and Physics, Changchun Institute of Applied Chemistry, and Graduate School of the Chinese Academy of Sciences, Chinese Academy of Sciences, Changchun 130022, People's Republic of China

Received October 15, 2004

The syntheses, structures, and electroluminescent properties are described for two new lanthanide complexes $Ln(HFNH)_3phen$ [HFNH = 4,4,5,5,6,6,6-heptafluoro-1-(2-naphthyl)hexane-1,3-dione; phen = 1,10-phenanthroline; Ln = Eu^{3+} (**1**), Sm^{3+} (**2**)]. Both complexes exhibit bright photoluminescence at room temperature (RT) due to the characteristic emission of Eu^{3+} and Sm^{3+} ion. Several devices using the two complexes as emitters were fabricated. The performances of these devices are among the best reported for devices using europium complex and samarium complex as emitters. The device based on **1** with the structure ITO/TPD (50 nm)/**1**:CBP (10%, 40 nm)/BCP (20 nm)/AlQ (30 nm)/LiF (1 nm)/Al (200 nm) exhibits the maximum brightness of 957 cd/m^2, current efficiency of 4.14 cd/A, and power efficiency of 2.28 lm/W with a pure red Eu^{3+} ion emission. Especially, at the high brightness of 200 cd/m^2, the device of **1** still has a high current efficiency of 2.15 cd/A. The device of **2** with a three-layer structure of ITO/TPD (50 nm)/**2** (50 nm)/BCP (20 nm)/LiF (1 nm)/Al (200 nm) gives the maximum brightness of 42 cd/m^2, current efficiency of 0.18 cd/A. By the comparison of the electroluminescent properties of devices based on $Eu(TTA)_3phen$ (TTA = 2-thenoyltrifluoroacteonate) and **1**, we conclude that the polyfluoration on the alkyl group of the ligand and the introduction of the long conjugate naphthyl group into the ligand improve the efficiency of **1**-doped devices, especially at high current densities.

Introduction

It is known that organic lanthanide complexes show promising properties as phosphors in thin-film organic electroluminescent (EL) displays.[1–9] Although organic light-emitting diodes (OLEDs) have attracted intense research interest in the development of full-color flat panel display devices, three main issues remain to be addressed: emission color, emission efficiency, and device lifetime. Organolanthanide complexes can provide potential solutions for the former two issues. First, the central lanthanide metal ions exhibit extremely sharp emission bands due to their 4f electrons. Next, internal quantum efficiencies are not a limitation (theoretically up to 100%) because both the singlet and the triplet are involved in the luminescence process.[8] Europium complexes have been characterized by highly efficient intraenergy conversion from the ligand singlet (S_1) to the ligand triplet (T_1), and thence to the excited state of the central lanthanide metal ion. The Eu^{3+} ions exhibit sharp spectral bands corresponding to $^5D_J \rightarrow {}^7F_J$ transitions. This mechanism is characterized by a high photoluminescence efficiency (20−95%) for europium complexes both in the

* Author to whom correspondence should be addressed. E-mail: hongjie@ciac.jl.cn.
† Changchun Institute of Applied Chemistry.
‡ Graduate School of the Chinese Academy of Sciences.

(1) Kido, J.; Hayase, H.; Hongawa, K.; Nagai K.; Okuyama, K. *Appl. Phys. Lett.* **1994**, *65*, 2124.
(2) Wang, K. Z.; Li, L. J.; Liu, W. M.; Xue, Z. Q.; Huang, C. H.; Lin, J. H. *Mater. Res. Bull.* **1996**, *31*, 993.
(3) Li, W. L.; Yu, J. Q.; Sun, G.; Hong, Z. R.; Yu, Y.; Zhao, Y.; Peng, J. B.; Tsutui, T. *Synth. Met.* **1997**, *91*, 263.
(4) Capecchi, S.; Renault, O.; Moon, D.-G.; Halim, M.; Etchells, M.; Dobson, P. J.; Salata, O. V.; Christou, V. *Adv. Mater.* **2000**, *12*, 1591.
(5) Xin, H.; Li, F. Y.; Shi, M.; Bian, Z. Q.; Huang, C. H. *J. Am. Chem. Soc.* **2003**, *125*, 7166.
(6) Zheng, Y. X.; Fu, L. S.; Zhou, Y. H.; Yu, J. B.; Yu, Y. N.; Wang, S. B.; Zhang, H. J. *J. Mater. Chem.* **2002**, *12*, 919.
(7) Adachi, C.; Baldo, M. A.; Forrest, S. R. *J. Appl. Phys.* **2000**, *87*, 8049.
(8) Kido, J.; Okamot, Y. *Chem. Rev.* **2002**, *102*, 2357 and references therein.
(9) Sun, P. P.; Duan, J. P.; Shih, H. T.; Cheng, C. H. *Appl. Phys. Lett.* **2002**, *81*, 792.

10.1021/ic0485561 CCC: $30.25
Published on Web 02/09/2005

solid state and in organic solution.[10−14] Because both singlet and triplet excitons are involved in the luminescence process, very high lanthanide ion excitation efficiency can be achieved by optimizing energy transfer in solid-state systems where the molecule is doped into an appropriate molecular host matrix.[7,9,15−17]

The central Eu^{3+} ions coordinated with β-diketone ligands give stronger and higher efficient fluorescence than that of the parent compounds (e.g., chloride, hydrate, etc.), especially when β-diketone ligands with aromatic or fluorine substituents are present.[13c−f,14] However, regular lanthanide β-diketone chelates have poor carrier-transport ability and cannot satisfy the need of fabricating OLEDs. To improve the carrier-transport properties of lanthanide complexes, two ways of modification have been made: one is introducing the charge-transport groups to ligands;[9,16−23] the other is doping lanthanide complexes into good carrier materials.[7,9,15−18] Seen from some relevant reports, devices based on Eu complexes without doping show high brightness, but do not have high efficiency. In contrast, devices based on Eu complexes doped into carrier materials show not only high brightness but also high efficiency. To improve the EL performance of OLEDs, some researchers have made chemical modification on the ligands of lanthanide complexes and obtained good results.[9,17−23] Seen from previous reports, fluorinated substituent in ligand increases the volatility of the complex, thus facilitating thin-film fabrication, and leads to improved thermal and oxidative stability and reduced concentration quenching of the luminescence.[24,25] Furthermore, fluorination can improve the PL and EL efficiency and enhance luminescence intensity.[25b,26] McGehee et al. chose different ligand substituents of Eu complex to study the performance of the OLEDs based on Eu β-diketone complex:CN−PPP-doped system as emitters.[15] They found that the efficiency was higher for the Eu complex whose ligand had longer conjugation lengths, that is, the complex with naphthyl substituent had a higher efficiency than those with other substituents (e.g., phenyl or methyl).

Herein, we have synthesized a new β-diketone ligand, which has the polyfluorinated alkyl group as well as the long conjugate naphthyl group. The EL devices based on the two lanthanide (Eu^{3+} and Sm^{3+}) complexes with this fluorinated β-diketone ligand show promising properties. We selected complex $Eu(HFNH)_3phen$ (**1**) as the emitter and CBP (4,4′-*N*,*N*′-dicarbazole-biphenyl) as the host because complex **1** can be sublimed in a vacuum without decomposition and CBP has a wide energy gap which supports bipolar carrier transport.[7,28] One of the devices based on **1** with the structure of ITO/TPD (50 nm)/**1**:CBP (10%, 40 nm)/BCP (20 nm)/AlQ (30 nm)/LiF (1 nm)/Al (200 nm) exhibits the maximum brightness of 957 cd/m^2, current efficiency of 4.14 cd/A, and power efficiency of 2.28 lm/W. In addition, this device shows a pure red Eu^{3+} ion emission at all current densities. It should be pointed out that the device of **1** still has a high current efficiency of 2.15 cd/A at the high brightness of 200 cd/m^2. The device of **2** with a three-layer structure of ITO/TPD (50 nm)/**2** (50 nm)/BCP (20 nm)/LiF (1 nm)/Al (200 nm) gives the maximum brightness of 42 cd/m^2, current efficiency of 0.18 cd/A. By the comparison in the performance of the device based on $Eu(TTA)_3phen$ and the device based on $Eu(HFNH)_3phen$, we conclude that the introduction of the polyfluorinated alkyl group and the long conjugate naphthyl group into the β-diketone ligand results in high EL efficiency of the devices based on the $Eu(HFNH)_3phen$ complex even at high current densities and at high brightness.

Experimental Section

Materials. Europium oxide (Eu_2O_3, 99.99%) and samarium oxide (Sm_2O_3, 99.99%) were purchased from Yue Long Chemical Plant (Shanghai, China). Metal sodium (≥98%, A. R.) and 1,10-phenanthroline monohydrate (phen·H_2O, 99%, A. R.) were purchased from Beijing Fine Chemical Co. (Beijing, China), 2′-acetonaphthone was from Acros Chemical Co. (Geel, Belgium), and ethyl heptafluorobutyrate was from Aldrich Chemical Co. (Milwaukee, WI). All of these reagents were used directly without further purification. $EuCl_3$ and $SmCl_3$ ethanol solutions were prepared using a literature procedure.[26]

Synthesis of Ligand HFNH. A modified method of a typical Claisen condensation procedure is used as follows. Metal sodium thread (0.276 g, 0.012 mol) was added into dry anhydrous ethanol

(10) (a) Whan, R. E.; Crosby, G. A. *J. Mol. Spectrosc*. **1962**, *8*, 315. (b) Bhaumik, M. L.; El-Sayed, M. A. *J. Chem. Phys.* **1965**, *42*, 787. (c) Malta, O. L.; Brito, H. F.; Menezes, J. F. S.; Gonqalves e Silva, F. R.; Alves, S., Jr.; Farias, F. S., Jr.; de Andrade, A. V. M. *J. Lumin.* **1997**, *75*, 255. (d) Malta, O. L.; Brito, H. F.; Menezes, J. F. S.; Gonqalves e Silva, F. R.; de Mello Donega, C.; Alves, A., Jr. *Chem. Phys. Lett.* **1998**, *282*, 233.

(11) (a) Taragin, M. F.; Eisenstein, J. C. *J. Inorg. Nucl. Chem.* **1973**, *35*, 3815. (b) Rikken, G. L. J. A. *Phys. Rev. A* **1995**, *51*, 4906.

(12) Sinha, S. P. *Complexes of the Rare Earth*; Progamon: London, 1966.

(13) (a) Wessiman, S. I. *J. Chem. Phys.* **1942**, *10*, 214. (b) Whan, R. E.; Corsy, G. A. *J. Mol. Spectrosc.* **1962**, *8*, 315. (c) Melby, L. R.; Rose, N. J.; Abramson, E.; Caris, J. C. *J. Am. Chem. Soc.* **1964**, *86*, 5117. (d) Bauer, H.; Blanc, J.; Ross, D. L. *J. Am. Chem. Soc.* **1964**, *86*, 5125. (e) Sager, W. F.; Filipescu, N.; Seraflin, F. A. *J. Phys. Chem.* **1965**, *69*, 1092. (f) Charlis, R. G.; Riedel, E. P. *J. Inorg. Nucl. Chem.* **1967**, *29*, 715. (g) Sato, S.; Wada, M. *Jpn. J. Appl. Phys.* **1968**, *7*, 7.

(14) Frey, S. T.; Gong, M. L.; W. D. H., Jr. *Inorg. Chem.* **1994**, *33*, 3229.

(15) McGehee, M. D.; Bergstedt, T.; Zhang, C.; Saab, A. P.; O'Regan, M. B.; Bazan, G. C.; Srdanov, V. I.; Heeger, A. J. *Adv. Mater*. **1999**, *11*, 1349.

(16) Noto, M.; Irie, K.; Era, M. *Chem. Lett.* **2001**, 320.

(17) (a) Fang, J. F.; Ma, D. G. *Appl. Phys. Lett.* **2003**, *83*, 4041. (b) Sun, P. P.; Duan, J.; Lih, J.; Cheng, C. *Adv. Funct. Mater.* **2003**, *13*, 683.

(18) Liang, C. J.; Zhao, D.; Hong, Z. R.; Zhao, D. X.; Liu, X. Y.; Li, W. L.; Peng, J. B.; Yu, J. Q.; Lee, C. S.; Lee, S. T. *Appl. Phys. Lett.* **2000**, *76*, 67.

(19) Wang, J.; Wang, R.; Yang, J.; Zheng, Z.; Carducci, M. D.; Cayon, T.; Peyghambarian, N.; Jabbour, G. E. *J. Am. Chem. Soc*. **2001**, *123*, 6179.

(20) (a) Okada, K.; Wang, Y. F.; Chen, T. M.; Kitamura, M.; Nakaya, T.; Inoue, H. *J. Mater. Chem.* **1999**, *9*, 3023. (b) Robinson, M. R.; O'Regan, M. B.; Bazan, G. C. *Chem. Commun.* **2000**, 1645.

(21) Sun, M.; Xin, H.; Wang, K. Z.; Zhang, Y. A.; Jin, L. P.; Huang, C. H. *Chem. Commun*. **2003**, 702.

(22) Xin, H.; Li, F. Y.; Guan, M.; Huang, C. H.; Sun, M.; Wang, K. Z.; Zhang, Y. A.; Jin, L. P. *J. Appl. Phys.* **2003**, *94*, 4729.

(23) Liang, F. S.; Zhou, Q. G.; Cheng, Y. X.; Wang, L. X.; Ma, D. G.; Jing, X. B.; Wang, F. S. *Chem. Mater*. **2003**, *15*, 1935.

(24) Omary, M. A.; Rawashdeh-Omary, M. A.; Diyabalanage, H. V. K.; Dias, H. V. R. *Inorg. Chem.* **2003**, *42*, 8612.

(25) (a) Grushin, V. V.; Herron, N.; LeCloux, D. D.; Marshall, W. J.; Petrov, V. A.; Wang, Y. *Chem. Commun.* **2001**, *16*, 1494. (b) Lasker, I. R.; Chen, T.-M. *Chem. Mater*. **2004**, *16*, 111.

(26) Zheng, Y. X.; Lin, J.; Liang, Y. J.; Lin, Q.; Yu, Y. N.; Meng, Q. G.; Zhou, Y. H.; Wang, S. B.; Wang, H. Y.; Zhang, H. J. *J. Mater. Chem.* **2001**, *11*, 2615.

(27) Kanai, H.; Ichinosawa, S. Y. *Synth. Met*. **1997**, *91*, 195.

(28) Rohatgi, K. K. *J. Sci. Ind. Res.* **1965**, *24*, 456.

(20 mL). The reaction mixture was stirred for 30 min at room temperature, after which 2′-acetonaphthone (1.702 g, 0.01 mol) and ethyl heptafluorobutyrate (2.905 g, 0.012 mol) were added. The mixture was then stirred for 48 h at room temperature. The resulting mixture was acidified to pH = 2−3 using hydrochloric acid (2 M solution), and the solvent was removed under reduced pressure at 70 °C. Acetone (30 mL) was added to the resulting mixture and stirred for 10 min. The mixture was filtered and washed with acetone several times (3 × 15 mL). The filtrate was collected, and the solvent was removed under reduced pressure to obtain a maroon oil, which was purified by chromatography on a silica gel column with hexane as the eluent to get a maroon liquid (2.930 g, 0.08 mol, yield of 80% based on 2′-acetonaphthone). ^{1}H NMR ($CDCl_3$, 400 MHz): δ, 6.76 (s, 1H), 7.61 (td, 1H, J = 8.0, 1.2 Hz), 7.65 (td, 1H, J = 8.0, 1.2 Hz), 7.90 (d, 1H, J = 8.0 Hz), 7.95−7.93 (m, 2H), 8.00 (d, 1H, J = 8.0 Hz), 8.54 (s, 1H), 15.38 (broad, 1H). Anal. Calcd for $C_{16}H_9F_7O_2$: C, 52.47; H, 2.48. Found: C, 52.70; H, 2.59.

Synthesis of Ln(HFNH)$_3$phen [Ln = Eu^{3+} (1), Sm^{3+} (2)]. Sodium hydroxide solution (1.0 M, 6.0 mL) was added dropwise to a mixture of HFNH (1.831 g, 6.0 mmol) and phen·H_2O (0.396 g, 2.0 mmol) in ethanol (20 mL) under stirring. $LnCl_3$ ethanol solution (0.195 M, 2.0 mmol) prepared separately was then added dropwise into this mixture. The mixture was heated to reflux and kept for 12 h at 80 °C. The resulting mixture was filtered and washed with water several times to give a solid product, which was dried under vacuum at 80 °C for 12 h, and then purified by recrystallization from an acetone/ethanol (V/V = 1:20) solution. The yields are 83% and 81% for **1** and **2**, respectively. Yellowish orange crystals (for **1**) and yellowish crystals (for **2**) suitable for X-ray single-crystal structural determination were grown from ethanol solutions. Anal. Calcd for $C_{60}H_{32}F_{21}N_2O_6Eu$: C, 50.47; H, 2.26; N, 1.96. Found: C, 50.36; H, 2.17; N, 1.91. Anal. Calcd for $C_{60}H_{32}F_{21}N_2O_6Sm$: C, 50.53; H, 2.26; N, 1.96. Found: C, 50.39; H, 2.21; N, 1.91.

X-ray Diffraction Analyses. Crystallographic data of **1** were collected at 298 K on a Siemens P4 diffractometer equipped with graphite monochromatic Mo Kα radiation (λ = 0.71073 Å). Intensity data were collected in the range of $3° \le 2\theta \le 50°$ by the ω scan techniques and corrected for Lorentz and absorption effects (ψ-scan). Three standard reflections were monitored every 97 reflections and showed no systematic changes. Data for **2** were recorded at room temperature (298 K) on a Bruker-AXS Smart CCD diffractometer equipped with a normal-focus, 2.4 kW sealed tube X-ray source (graphite-monochromated Mo Kα radiation with λ = 0.71073 Å) operating at 50 kV and 40 mA. Intensity data were collected in 1271 frames with increasing ω (width of 0.3° and exposure time 30 s per frame). An absorption correction was made using the SADABS program (T_{max} = 0.3282 and T_{min} = 0.1718). The structures were solved by direct method using SHELXS-97 and refined by full-matrix least-squares techniques against F^2 using the SHELXL-97 program package. Non-hydrogen atoms (for **1** except F atoms, for **2** except F5−F7; F12−F21; F26−F35; F41−42 atoms) were refined anisotropically. All of the hydrogen atoms were generated manually based on idealized geometries.

Instrumentation. The ^{1}H NMR spectra were recorded on a Bruker DRX 400 spectrometer. Element analyses were performed using a Vario Element Analyzer. UV−vis absorbance spectra were recorded using a TU 1901 UV−vis spectrophotometer. The photoluminescence (PL) spectra were measured on a Hitachi F-4500 fluorescence spectrophotometer. The electroluminescence (EL) spectra were measured on a JY SPEX CCD3000 spectrometer. Current density−brightness−voltage (J−B−V) characteristics were measured using a Keithley source measurement unit (Keithley 2400 and Keithley 2000) with a calibrated silicon photodiode. All measurements were carried out in ambient atmosphere at room temperature. The TGA-DTA analyses were measured using an SDT 2960 Simultaneous DSC-TGA of TA instruments, and the heating rate was 10 °C/min.

Scheme 1. Synthetic Route to Complexes **1** and **2**[a]

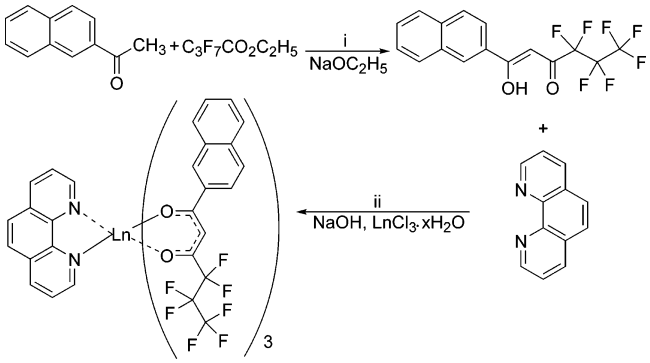

[a] (i) Room temperature, stirred 48 h; (ii) 80 °C, reflux 12 h.

Table 1. Crystal Data and Structure Refinement for **1** and **2**

	1	2
empirical formula	$C_{60}H_{32}F_{21}N_2O_6Eu$	$C_{60}H_{32}F_{21}N_2O_6Sm$
fw	1427.84	1426.23
temp	293(2) K	293(2)K
radiation, wavelength	Mo Kα 0.71073 Å	Mo Kα 0.71073 Å
crystal system	triclinic	triclinic
space group	$P\bar{1}$	$P\bar{1}$
a (Å)	11.700 (3)	11.6777 (4)
b (Å)	21.111 (8)	21.1704 (8)
c (Å)	24.369 (9)	24.3540 (8)
α (deg)	76.39 (3)	76.475 (2)
β (deg)	86.47 (3)	86.661 (2)
γ (deg)	88.36 (3)	88.435 (2)
V (Å^3)	5839 (3)	5843.3 (4)
Z	4	4
ρ_{calc} (Mg/m^3)	1.625	1.621
μ (mm^{-1})	1.194	1.124
F (000)	2824	2820
θ range (deg)	1.72−25.10	1.46−25.00
reflns collected	24 145	19 083
independent reflns	20 497	10 736
final R [$I > 2\sigma(I)$]	R1 = 0.0828	R1 = 0.0696
	wR2 = 0.1596	wR2 = 0.1686
R indices (all data)	R1 = 0.2243	R1 = 0.1265
	wR2 = 0.1918	wR2 = 0.2014

Fabrication of EL Devices. The EL devices with lanthanide complexes as the emitting layer were fabricated on an indium−tin oxide (ITO) substrate, which was cleaned by a lotion from a French company (FRANKLAB S. A.) specifically made for rinsing ITO glass plates, followed by anhydrous ethanol. The organic layers were sequentially deposited at a rate in the range of 0.1−0.3 nm/s under high vacuum ($\le 8 \times 10^{-5}$ Pa). At last, LiF layer and Al layer were deposited at a rate of 0.05 and 0.8−1.0 nm/s, respectively, under the same high vacuum. The thickness of the deposited layer and the evaporation speed of the individual materials were monitored in a vacuum with quartz crystal monitors. The active device area was 10 mm^2.

Results and Discussion

Syntheses and Structures of 1 and 2. The whole synthetic procedure of lanthanide complexes is shown in Scheme 1. Both the ligand HFNH and the lanthanide complexes (**1**, **2**) were prepared by typical methods. The

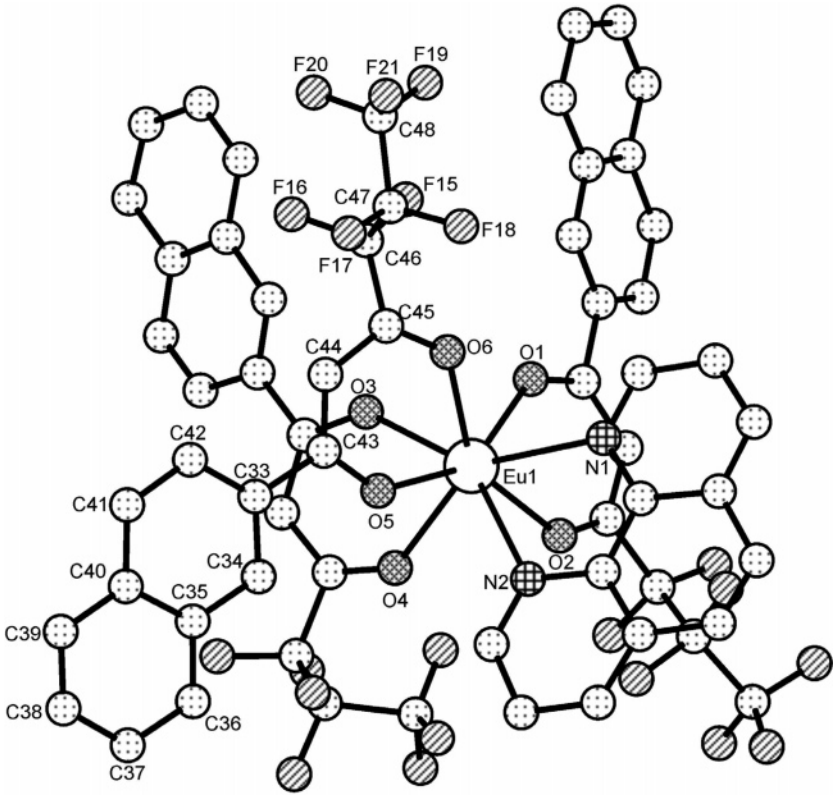

Figure 1. Perspective view showing the asymmetric unit of complex **1** with the atom labeling schemes. Hydrogen atoms were omitted for clarity.

second added ligand, phen, is coordinated with Ln^{3+} ions as a synergic agent, which not only saturates the coordination number of the Ln^{3+} ions, but also improves the fluorescence intensity, volatility, and stability of the lanthanide complex.[8,14,28] This further step enhances the luminescent intensity of lanthanide complexes (**1**, **2**) and makes them more sublimable. Complexes **1** and **2** are stable in air and soluble in common organic solvents, such as CH_2Cl_2, $CHCl_3$, acetone, and ethyl acetate, but insoluble in water.

Single-crystal X-ray diffraction studies revealed similar crystal structures for complexes **1** and **2**, whose crystals fall in the same centrosymmetric space group. The crystallographic data of **1** and **2** are given in Table 1. There are two independent molecules in the asymmetric unit of both **1** and **2**. The structures of these two independent molecules of **1** are similar, one of which is shown in Figure 1. The corresponding selected bond lengths and angles are given in Table 2. In complexes **1** and **2**, each central Ln^{3+} ion is coordinated by six oxygen atoms from three HFNH ligands and two nitrogen atoms from phen ligand, resulting in a coordination number of eight for each central metal ion. The coordination geometry of the metal can be described as a distorted square antiprism with six oxygen atoms and two nitrogen atoms.

PL Properties of Complexes 1 and 2. The absorption, excitation, and emission spectra of complexes **1** and **2** were shown in Figure 2. The absorption spectra were measured in ethanol solution (1×10^{-4} M). The excitation and emission spectra were measured from the solid states. Both the absorption and the excitation spectra are broad bands from 200 to 450 nm mainly attributed to the absorption and

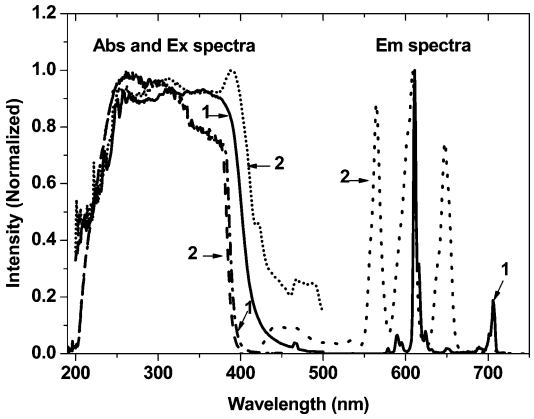

Figure 2. UV−vis absorption (**1**, dash dot; **2**, dash), excitation (**1**, solid, $\lambda_{em} = 611$ nm; **2**, short dot, $\lambda_{em} = 608$ nm), and emission (**1**, solid, $\lambda_{ex} = 356$ nm; **2**, dot, $\lambda_{ex} = 390$ nm) spectra of **1** and **2**.

excitation of ligands HFNH and phen. Seen from Figure 2, the excitation spectra of two complexes overlap well within the absorbance wavelength range, indicating that the emissions originate from the energy absorbed by the ligands. Complexes **1** and **2** show strong red (for **1**) and reddish-orange (for **2**) luminescence in solution and solid state when irradiated by UV light. When excited by light at 356 nm, the emission spectrum of **1** consists of entirely characteristic emission bands of Eu^{3+} ion ($^5D_0 \rightarrow {}^7F_J$, $J = 0, 1, 2, 3, 4$). However, the emission (excited at 390 nm) of **2** exhibits not only characteristic emission of Sm^{3+} ($^5G_{5/2} \rightarrow {}^6H_J$, $J = 3/2$, 5/2, 7/2, 9/2, 11/2), but also a weaker wide emission band (420−480 nm) of the ligand HFNH. Generally, organolanthanide complex emission is originated from the excitation of ligands. Through intersystem crossing, the energy is

Table 2. Selected Bond Lengths and Angles for One of the Molecules of **1** and **2**

	1	2
Ln(1)−O(1)	2.342(9)	2.370(10)
Ln(1)−O(3)	2.345(9)	2.364(9)
Ln(1)−O(4)	2.347(10)	2.366(10)
Ln(1)−O(6)	2.359(10)	2.388(11)
Ln(1)−O(5)	2.370(9)	2.394(10)
Ln(1)−O(2)	2.397(9)	2.417(11)
Ln(1)−N(1)	2.585(11)	2.596(11)
Ln(1)−N(2)	2.606(11)	2.603(11)
O(1)−Ln(1)−O(3)	76.6(3)	77.0(3)
O(1)−Ln(1)−O(4)	119.9(3)	119.5(4)
O(3)−Ln(1)−O(4)	72.0(3)	71.7(3)
O(1)−Ln(1)−O(6)	83.0(3)	82.2(4)
O(3)−Ln(1)−O(6)	78.2(3)	78.2(3)
O(4)−Ln(1)−O(6)	135.5(3)	136.3(4)
O(1)−Ln(1)−O(5)	149.7(3)	150.3(4)
O(3)−Ln(1)−O(5)	84.5(3)	85.1(3)
O(4)−Ln(1)−O(5)	74.9(3)	75.6(4)
O(6)−Ln(1)−O(5)	70.0(3)	70.9(3)
O(1)−Ln(1)−O(2)	70.9(3)	70.5(4)
O(3)−Ln(1)−O(2)	113.4(3)	113.1(4)
O(4)−Ln(1)−O(2)	76.6(3)	76.2(4)
O(6)−Ln(1)−O(2)	146.9(3)	146.3(4)
O(5)−Ln(1)−O(2)	139.3(3)	139.0(3)
O(1)−Ln(1)−N(1)	76.9(3)	78.1(4)
O(3)−Ln(1)−N(1)	145.3(3)	146.8(3)
O(4)−Ln(1)−N(1)	141.8(4)	140.7(4)
O(6)−Ln(1)−N(1)	76.7(4)	77.0(4)
O(5)−Ln(1)−N(1)	108.6(3)	106.9(4)
O(2)−Ln(1)−N(1)	77.9(3)	78.2(4)
O(1)−Ln(1)−N(2)	131.5(4)	131.3(4)
O(3)−Ln(1)−N(2)	149.1(4)	148.7(3)
O(4)−Ln(1)−N(2)	80.9(4)	80.8(3)
O(6)−Ln(1)−N(2)	113.5(4)	114.3(4)
O(5)−Ln(1)−N(2)	74.1(3)	73.4(3)
O(2)−Ln(1)−N(2)	73.2(3)	73.2(4)
N(1)−Ln(1)−N(2)	64.6(4)	63.4(4)

transferred from the singlet state S_1 to the triplet state T_1 in the ligand. The ligand then intramolecularly transfers energy from its lowest excited triplet state to the excited states of the central lanthanide ion.[6,8] Finally, the central ion gives fluorescence through radiative transition from the excited state to the ground state. The results shown in Figure 2 indicate that a complete internal conversion occurred from the ligand to the central Eu^{3+} ions in complex **1**, but this is not the case for complex **2** where the internal conversion is incomplete. According to Sato et al.,[29] to improve energy transfer probability from the triplet state of the ligand to the resonance level of Ln^{3+} ion, the triplet state of the ligand must be closely matched to or slightly above the metal ion's emitting resonance levels. In fact, the energy level $^5G_{5/2}$ of Sm^{3+} (18 000 cm^{-1})[30] is higher than the energy level $^5D_0$ of Eu^{3+} (17 500 cm^{-1}).[29] Possibly, the triplet state of HFNH ligand is not matched to Sm^{3+} ion's emitting resonance levels $^5G_{5/2}$. As stated above, a weak ligand emission band appears in the emission spectrum of **2** due to incomplete energy transfer.

EL Properties of Complexes 1 and 2. The TGA-DTA analyses show that the melting points of **1** and **2** are 172 and 114 °C, respectively, and the decomposition temperatures are 379 and 389 °C, respectively. The results indicate that

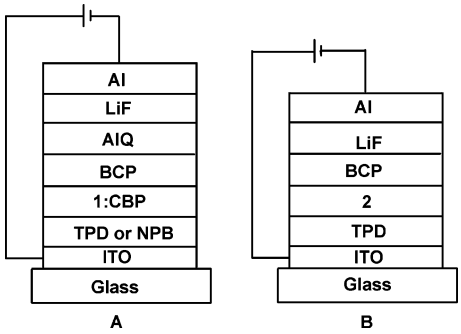

Figure 3. General structure of the devices: **A**, type of device for europium, ITO/TPD or NPB/Eu complex, CBP/BCP/AlQ/LiF/Al; **B**, type of device for samarium, ITO/TPD (50 nm)/**2** (50 nm)/BCP (20 nm)/LiF (1 nm)/Al (200 nm).

two complexes have good thermal stability and can be sublimed at low temperature due to fluorination on β-diketone ligands. For europium complexes, the doping method was often used to fabricate devices to improve efficiency. Because CBP has a wide energy gap which supports bipolar carrier transport[7,28] and europium β-diketone complexes generally have low-lying highest occupied molecular orbital levels due to relatively high oxidative state of europium ion,[9] we can fabricate several devices using CBP as the host and **1** as the guest. The general structure of the dopant devices based on **1** as the emitter is shown in Figure 3. Here, TPD (4,4′-bis[*N*-(*p*-tolyl)-*N*-phenyl-amino]biphenyl) or NPB (4,4′-bis[*N*-(1-naphthyl)-*N*-phenyl-amino]biphenyl) serves as the hole transporter, whereas AlQ (tris[8-hydroxyquinoline]) and BCP (2,9-dimethyl-4,7-diphenyl-1,10-phenanthroline) are used as electron transporters. Thus, TPD (or NPB) and BCP can confine electrons and holes effectively in the emitting layer. A layer of CBP doped with **1** at different concentration serves as the emitter between the layer of TPD and BCP.

Forrest et al.[7] reported that excited CBP singlet energies were partially transferred to $Eu(TTA)_3$phen singlet states via a Förster process when the Eu complex is doped into CBP. Herein, we studied the PL properties of the **1**:CBP system where the dopant concentration of **1** in CBP dissolved in CH_2Cl_2 was varied from 1% to 20%. The CH_2Cl_2 solution was spin-coated onto quartz substrate to form films for spectroscopy. The spectra shown in Figure 4 a indicate that an overlap between CBP fluorescence and **1** absorption is only significant between $\lambda = 300-400$ nm. From the PL spectra (Figure 4b), an emission from CBP in the PL spectrum of **1**:CBP can be always observed despite the high dopant concentration of **1** (up to as high as 20%). All of these results show that the energy transfer from CBP to **1** via a Förster process is inefficient, as reported in some other references.[7,9] When the dopant concentration of **1** was 5%, the CBP emission became weak in the PL spectra of the **1**:CBP system. We also found that there was no obvious concentration quenching of Eu complex luminescence until the dopant concentration of **1** was 20%.

To understand the EL performance of **1** as red emitters in EL devices, we fabricated several devices with the device configuration shown in Figure 3A using **1** as dopant emitters with concentrations from 1% to 15%. Key characteristics of some devices are listed in Table 3. Devices with dopant

(29) Sato, S.; Wada, M. *Bull. Chem. Soc. Jpn.* **1970**, *43*, 1955.
(30) Rosriguez, V. D.; Martin, I. R.; Alcata, R.; Cases, R. *J. Lumin.* **1992**, *54*, 231.

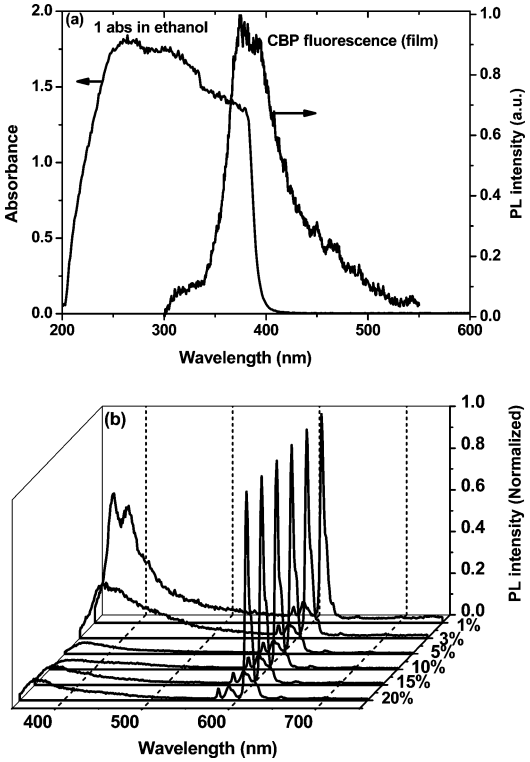

Figure 4. (a) The absorption spectrum of 10^{-5} M **1** in ethanol solution. (b) PL spectra of **1**:CBP (1−20%) films (λ_{ex} = 254 nm).

Table 3. Performances of OLEDs Based on **1**[a]

device[b]	J[c] (mA/cm^2, V)	L (cd/m^2)	η_c (cd/A)	η_p (lm/W)
A	0.021, 4.9	1	4.88	3.13
	12.3, 10.1	204	1.66	0.52
	389.7, 16.2	1013	0.26	0.05
B	0.034, 5.4	1	3.04	1.77
	11.6 13.9	201	1.74	0.39
	298.0, 18.4	819	0.27	0.05
C	0.026, 5.7	1	4.14	2.28
	9.3, 15	200	2.15	0.44
	305.3, 19.1	957	0.31	0.05
D	0.035, 6.3	1	3.56	1.77
	9.9, 16.4	203	2.25	0.43
	259.9, 22	1132	0.48	0.07
E	0.031, 7.5	1	3.31	1.39
	18.1, 18.7	203	1.11	0.19
	266.4, 22.8	856	0.32	0.04
F	0.050, 5.7	1	1.98	1.09
	13.1, 14.8	206	1.57	0.33
	301.4, 20.2	1062	0.35	0.05
G	0.035, 5.2	1	3.36	2.02
	10.1, 15.6	205	2.23	0.45
	296.9, 21.4	1121	0.42	0.06

[a] Luminance (L), current efficiency (η_c), and power efficiency (η_p) are given as functions of current density. [b] Device **A**, TPD (50 nm)/**1**:CBP (9%, 40 nm)/BCP (20 nm)/AlQ (30 nm); device **B**, TPD (50 nm)/**1**:CBP (10%, 30 nm)/BCP (20 nm)/AlQ (30 nm); device **C**, TPD (50 nm)/**1**:CBP (10%, 40 nm)/BCP (20 nm)/AlQ (30 nm); device **D**, TPD (50 nm)/**1**:CBP (10%, 40 nm)/BCP (25 nm)/AlQ (30 nm); device **E**, NPB (50 nm)/**1**:CBP (10%, 40 nm)/BCP (20 nm)/AlQ (30 nm); device **F**, TPD (50 nm)/**1**:CBP (11%, 30 nm)/BCP (20 nm)/AlQ (30 nm); device **G**, TPD (50 nm)/**1**:CBP (8%, 40 nm)/BCP (20 nm)/AlQ (30 nm). [c] Current density (J) is given when L is about 1 cd/m^2, 200 cd/m^2, and the maximal data.

concentrations < 9% showed undesirable CBP (λ_{max} = 400 nm) and BCP (λ_{max} = 500 nm) emissions besides characteristic red emission of Eu^{3+} ion (one of the spectra shown in Figure 5, **G** 19V). Weak emission from AlQ (λ_{max} = 520 nm) was observed in the EL spectra, especially at high current densities when the dopant concentration of complex **1** was increased to 12%. The same results were also observed when the dopant concentration was increased to 13% and 15%. The reason is that high concentration can induce concentration quenching of the luminescence of **1**. With the appropriate concentration (9−11%), the emissions from CBP and BCP were efficiently quenched in devices **A**−**F**, and these devices showed pure red emission of Eu^{3+} ion ($^5D_0 \rightarrow {}^7F_J$, J = 0, 1, 2, 3, 4) centered at λ = 611 nm with a full width at half-maximum of 3 nm at all current densities (shown in Figure 5). Devices **A**, **B**, **C**, and **F** had maximum brightness between 819 and 1062 cd/m^2, current efficiency in the range of 2.73−4.88 cd/A, and power efficiency in the range of 1.24−3.13 lm/W, and had the current efficiency in the range of 1.57−2.15 cd/A at the brightness of 200 cd/m^2. Among the four devices **A**, **B**, **C**, and **F**, device **C** with a dopant concentration of 10% showed the best device performance especially at the brightness of 200 cd/m^2. The highest current efficiency of 4.14 cd/A, power efficiency of 2.28 lm/W, and brightness of 957 cd/m^2 were obtained. Furthermore, the highest current efficiency of 2.15 cd/A (shown in Table 3) was achieved at the brightness of 200 cd/m^2, which is crucial for practical application of OLEDs.

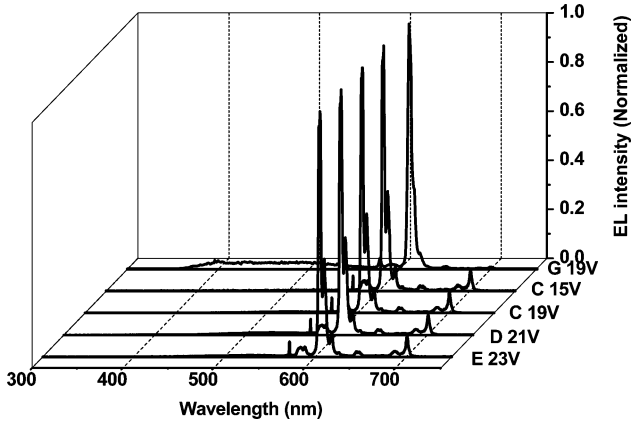

Figure 5. The EL spectra of several devices based on **1**, device **C** at 15 and 19 V, device **D** at 21 V, device **E** at 23 V, and device **G** at 19 V.

In addition to the dopant concentration, the thickness of both the emitting layer and the BCP layer also affected the performances of devices. Decreasing the thickness of the emitting layer from 40 nm (in device **C**) to 30 nm (in device **B**) not only decreased the turn-on voltage from 5.7 to 5.4 V but also decreased the maximum current efficiency from 4.14 to 3.48 cd/A, power efficiency from 2.28 to 1.85 lm/W, and brightness from 957 to 819 cd/m^2. When the BCP layer was increased from 20 nm (in device **C**) to 25 nm (in device **D**), the maximum brightness increased to 1132 cd/m^2, but the current efficiency and power efficiency of device **D** decreased to 3.56 cd/A and 1.77 lm/W, respectively. The turn-on voltage was also increased from 5.7 to 6.3 V. However, we also observed that device **D** showed higher current efficiency than device **C** at high current densities (>10 mA/cm^2, in Figure 6). This indicates that the thicker BCP layer can effectively confine carriers in the emitting layer, especially at high current densities.

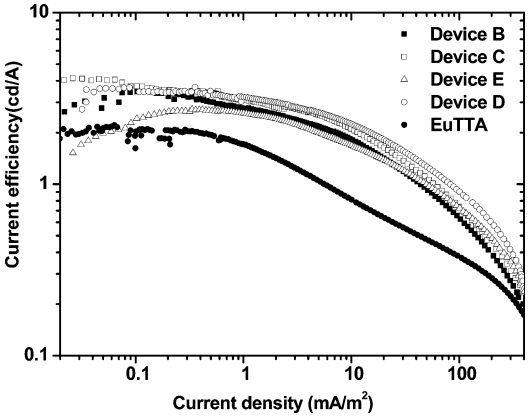

Figure 6. The current efficiency versus current density characteristics due to different devices based on **1**:CBP as emitter of (i) device **A**, (ii) device **C**, (iii) device **D**, (iv) device **E**, and (vi) device based on Eu(TTA)$_3$phen (1%).

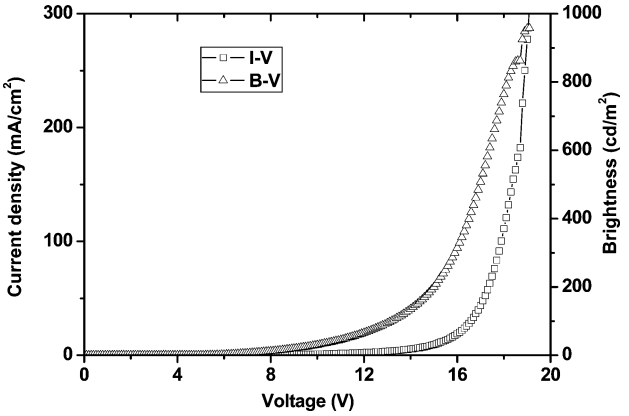

Figure 7. The current density−brightness−voltage characteristics of device **C**.

When TPD was replaced by NPB as a hole transporter for device **E** based on **1**, the device showed a maximum brightness of 856 cd/m^2, current efficiency of 4.1cd/A, and power efficiency of 1.48 lm/W. The current efficiency of device **E** decreased sharply as the current density increased. At the brightness of 203 cd/m^2 (18.1 mA/cm^2), the current efficiency was only 1.11 cd/A. Furthermore, the turn-on voltage was increased from 5.7 V (device **C**) to 7.5 V. In conclusion, device **C** exhibits the best EL properties with the structure of ITO/TPD (50 nm)/**1**:CBP (10%, 40 nm)/ BCP (20 nm)/AlQ (30 nm)/LiF (1 nm)/Al (200 nm). The current density−brightness−voltage (J−B−V) characteristics of device **C** are shown in Figure 7. A summary of performances of OLEDs based on europium complexes doped into CBP as the emitter in the literature is listed in Table 4. By comparison, we can see that the EL property of device **C** is among the best reported for devices with europium complexes as the emitter.[7,9,17a]

To investigate the effect of the polyfluorinated alkyl group and the long conjugate naphthyl group of the ligand HFNH on the performance of OLEDs based on complex **1**, we have fabricated several devices based on Eu(TTA)$_3$phen as the emitter with the dopant concentration varing from 1% to 5%. As reported,[7] there were always emissions from CBP observed with increasing current density in the EL spectra of devices with different structures (shown in Figure 8). The

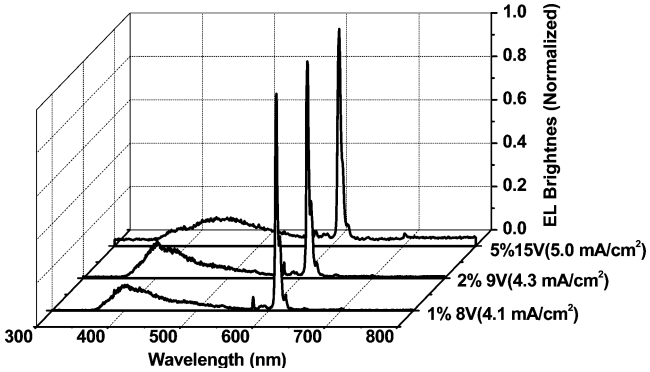

Figure 8. The EL spectra of several devices based on Eu(TTA)$_3$phen (1%, 2%, 5%).

Table 4. Summary of Europium Complex:CBP-Based OLEDs

emitter layer	L, V cd/m^2, V	η_c, J cd/A, mA/cm^2	η_p, J lm/W, mA/cm^2	ref
Eu(HFNH)$_3$phen (10%)	957, 19.1	4.14, 0.026	2.28, 0.026	this work
Eu(TTA)$_3$phen (1%)	505, 12.0			7
Eu(TTA)$_3$DPPZ (4.5%)	1670, 13.6	4.4, 1.23	2.1, 1.23	9
Eu(TTA)$_3$(Tmphen) (1%)	800, 24.5	4.7, 0.1	1.6, 0.1	17a

Table 5. Current Efficiency Comparison between the Devices Based on Eu(TTA)$_3$phen (1%) and **1** (10%)

	current efficiency (cd/A)		
device	1 mA/cm^2	10 mA/cm^2	50 mA/cm^2
Eu(TTA)$_3$phen (1%)	1.4	0.7	0.4
1 (10%, device **C**)	3.1	2.1	1.1

efficiency of the device was decreased with increasing dopant concentration. The best concentration was 1%, and the best device structure was ITO/TPD (50 nm)/Eu(TTA)$_3$phen:CBP (1%, 30 nm)/BCP (20 nm)/AlQ (30 nm)/LiF (1 nm)/Al (200 nm). The current efficiency of the device based on Eu(TTA)$_3$phen (1%) and the current efficiency of device **C** at different current densities are shown in Table 5. Seen from Table 5 and Figure 6, a significant decrease of current efficiency of the device based on Eu(TTA)$_3$phen (1%) was observed. The decrease of efficiency of the device based on Eu(TTA)$_3$phen-doped CBP with increasing current density was found to be due to T−T annihilation on CBP molecules following back transfer from ligand TTA due to the near resonance of TTA and CBP triplet.[7] However, such a significant decrease was not observed in device **C** which still had high current efficiency at high current density. A possible candidate for this result is that the high dopant concentration and the large ligand molecular volume (in contrast to ligand TTA) of **1** lengthen the distance between the adjacent CBP molecules, which diminishes the CBP T−T annihilation. It is the introduction of the polyfluorinated alkyl group and the long conjugate naphthyl group into the β-diketone ligand that has increased the dopant concentration and the molecular volume of **1**. Another possible mechanism that cannot be excluded is that the introduction of the polyfluorinated alkyl group and the long conjugate naphthyl group can lower the triplet state of HFNH ligand,[13g,26] which diminishes the back transfer of energy from HFNH to CBP. Last, fluorine atom

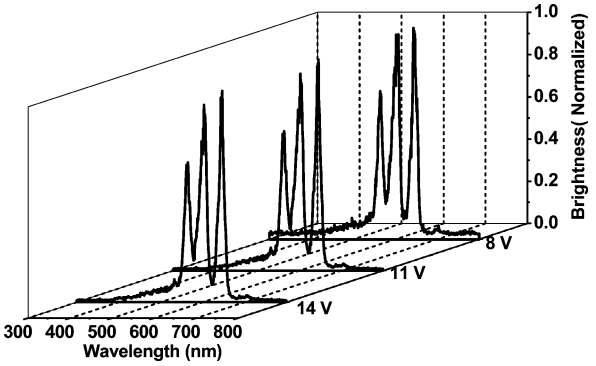

Figure 9. The EL spectra of a device based on **2** at different voltages.

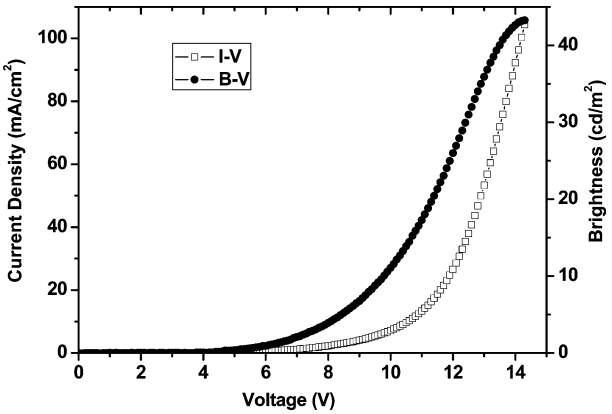

Figure 10. The *J*−B−V characteristics of a device based on **2**.

substituting hydrogen can lower the vibration energy of the ligand, which decreases the energy loss and enhances luminescence efficiency.[26]

We also observed that there was no emission from CBP in **1**-doped CBP devices (device **A**−**F**) at all current densities. However, there were always emissions from CBP in the PL spectra of the **1**:CBP system. The difference between PL spectra and EL spectra indicates that the carrier trapping is the main electroluminescence process. In this case, the injected electrons and holes through CBP are first trapped by complex **1**, and then form excitons on complex **1**. In addition, CBP singlet energies partially transferred to **1** singlet states via a Förster process may be included in the mechanism of the EL process of these devices.[7,9,17]

For complex **2**, we have also tried to dope it into the CBP host to fabricate devices. Although many structures of devices had been designed to fabricate devices based on **2**:CBP emitter, we failed to obtain devices with pure Sm^{3+} ion emission. There were always CBP emission ($\lambda = 400$ nm) and BCP emission ($\lambda = 500$ nm) besides the characteristic Sm^{3+} ion emission. So the device structure shown in Figure 3B was used to fabricate devices with complex **2** as the emitter, and BCP was used as the electron transporter. The device exhibited pure reddish-orange EL of characteristic Sm^{3+} ion emission ($^5G_{5/2} \rightarrow {}^6H_J$, $J = 3/2$, 5/2, 7/2, 9/2, 11/2). The three strongest emission bands were located at 563, 604, and 646 nm, corresponding to $^5G_{5/2} \rightarrow {}^6H_{5/2}$, $^5G_{5/2} \rightarrow {}^6H_{7/2}$, and $^5G_{5/2} \rightarrow {}^6H_{9/2}$ transitions, respectively (Figure 9). The *J*−B−V characteristics of **2**-based OLEDs are given in Figure 10. The device exhibits the maximum brightness of 43 cd/m^2 at 14 V ($J = 100$ mA/cm^2) and current efficiency of 0.18 cd/A, $J = 1.1$ mA/cm^2.

In conclusion, we have demonstrated the syntheses and structures of two new lanthanide (Eu^{3+}, Sm^{3+}) complexes. The devices based on them are also studied. The device with the structure of ITO/TPD (50 nm)/**1**:CBP (10%, 40 nm)/BCP (20 nm)/AlQ (30 nm)/LiF (1 nm)/Al (200 nm) emits pure red emission of Eu^{3+} ion centered at $\lambda = 611$ nm with a full width at half-maximum of 3 nm at all current densities and shows the maximum brightness of 957 cd/m^2, current efficiency of 4.14 cd/A, and power efficiency of 2.28 lm/W. At the brightness of 200 cd/m^2, the current efficiency remains as high as 2.15 cd/A. These values are among the best reported for devices based on Eu complexes as emitters. The device based on complex **2** exhibits the maximum brightness of 43 cd/m^2 at 14 V ($J = 100$ mA/cm^2) and current efficiency of 0.18 cd/A, $J = 1.1$ mA/cm^2. By the comparison in the performance of the device based on $Eu(TTA)_3phen$ and the device based on $Eu(HFNH)_3phen$, we conclude that the introduction of the polyfluorinated alkyl group and the long conjugate naphthyl group leads to the high EL efficiency of OLEDs based on the $Eu(HFNH)_3phen$ complex at high current densities and at high brightness. Our results demonstrate that the EL performance of OLEDs based on lanthanide complex can be effectively improved by chemical modification on the β-diketone ligand.

Acknowledgment. We are indebted to the National Natural Science Foundation of China (Nos. 20171043, 20372060, 20131010, 20121701), the "863" National Foundation for High Technology Development and Programming (Nos. 2002AA302105, 2002AA324080), and the Foreign Communion & Cooperation of National Natural Science Foundation of China (No. 20340420326). We are grateful to Professor Dongge Ma for his advice on the fabricating device process.

Supporting Information Available: Molecular structures of complexes **1** and **2**. Crystallographic data of complex **1** and **2** in CIF format. This material is available free of charge via the Internet at http://pubs.acs.org.

IC0485561